

**Phenylarsonic acid–DMPs redox reaction and conjugation investigated
by NMR spectroscopy and X-ray diffraction**

Kretzschmar, J.; Brendler, E.; Wagler, J.;

Originally published:

March 2022

Environmental Toxicology and Pharmacology 92(2022), 103837-103844

DOI: <https://doi.org/10.1016/j.etap.2022.103837>

Perma-Link to Publication Repository of HZDR:

<https://www.hzdr.de/publications/Publ-33657>

Release of the secondary publication
on the basis of the German Copyright Law § 38 Section 4.

CC BY-NC-ND

Phenylarsonic acid–DMPS redox reaction and conjugation investigated by NMR spectroscopy and X-ray diffraction

Jerome Kretzschmar,^{†1} Erica Brendler,^{†*} Jörg Wagler[‡]

[†]Institute of Analytical Chemistry, TU Bergakademie Freiberg, 09596 Freiberg, Germany.

[‡]Institute of Inorganic Chemistry, TU Bergakademie Freiberg, 09596 Freiberg, Germany.

Abstract

The reaction between 2,3-dimercaptopropane-1-sulfonate (DMPS, unithiol) and four phenylarsonic(V) acids, *i.e.* phenylarsonic acid (PAA), 4-hydroxy-3-nitrophenylarsonic acid (HNPA), 2-aminophenylarsonic acid (*o*-APAA) and 4-aminophenylarsonic acid (*p*-APAA), is investigated in aqueous solution. The pentavalent arsenic compounds are reduced by DMPS to their trivalent analogs and instantly chelated by the *vicinal* dithiol, forming covalent As–S bonds within a five-membered chelate ring. The different types and positions of polar substituents at the aromatic ring of the arsonic acids influence the reaction rates in the same way as observed for reaction with glutathione (GSH), as well as the *syn* : *anti* molar ratio of the diastereomeric products, which was analyzed using time- and temperature-dependent nuclear magnetic resonance (NMR) spectroscopy. Addition of DMPS to the conjugate formed by a phenylarsonic(V) acid and the biologically relevant tripeptide GSH showed the immediate replacement of GSH by chelating DMPS, underlining the importance of dithiols as detoxifying agent.

¹ Present Address: Helmholtz-Zentrum Dresden-Rossendorf e.V. (HZDR), Institute of Resource Ecology, Bautzner Landstr. 400, 01328 Dresden, Germany.

* Corresponding author at: TU Bergakademie Freiberg, Institute of Analytical Chemistry, Leipziger Str. 29, 09599 Freiberg, Germany. Email address: erica.brendler@chemie.tu-freiberg.de

Keywords

Arsenic; Unithiol; GSH; Molecular Structure; Kinetics; Toxicology.

Abbreviations

DMPS, 2,3-dimercaptopropane-1-sulfonate; GSH, glutathione, γ -L-glutamyl-L-cysteinyl-glycine; PAA, phenylarsonic acid; HNPA, 4-hydroxy-3-nitrophenylarsonic acid; *o*-APAA, 2-aminophenylarsonic acid; *p*-APAA, 4-aminophenylarsonic acid; BAL, British Anti-Lewisite, 2,3-dimercaptopropane-1-ol; PAO, phenylarsine oxide; DMSA, meso-2,3-dimercaptosuccinic acid; PDA, phenyldichloroarsine; PDT, 1,2-dimercaptopropane; NMR, Nuclear Magnetic Resonance; XRD, X-ray diffraction; NOESY, Nuclear Overhauser effect spectroscopy; EXSY, exchange spectroscopy; COSY, correlation spectroscopy; HSQC, heteronuclear single-quantum coherence; HMBC, heteronuclear multiple-bond correlation.

1. Introduction

Organoarsenic compounds play a crucial role in environmental contaminations caused by residues of arsenic containing chemical warfare agents (Leermakers et al., 2006; Niemikoski et al., 2020; Pitten et al., 1999; Stock, 1996; Stock and Lohs, 1997; Tørnes et al., 2006). Diphenylarsine chloride and cyanide, phenarsazine chloride, and phenylarsine dichloride were produced in large scale during the First and Second World War (Chauhan et al., 2008; Stock, 1996). At former military sites hydrolysis and oxidation products contaminate soils and waters resulting in high arsenic levels (Pitten et al., 1999). Other phenylarsenic compounds, especially 4-hydroxy-3-nitrophenylarsonic acid (HNPA, roxarsone) and 4-aminophenylarsonic acid (*p*-APAA) have been used as growth promoters and veterinary drugs in poultry and swine feed additives (Anderson, 1983; Czarnecki et al., 1984; D'Angelo et al., 2012; Pergantis et al., 1997; Sun et al., 2002). Additionally, various inorganic and organic arsenicals have been used for centuries or are still used in human medicine to treat diseases such as human trypanosomiasis (sleeping sickness), syphilis, or promyelocytic leukemia (Chen et al., 2015; Dilda and Hogg, 2007; Miller Jr et al., 2002).

Arsenic metabolism is of paramount interest and hence subject of current and ongoing research. Depending on speciation, tri- and pentavalent organic and inorganic arsenicals are associated with severe health effects, including the gastrointestinal as well as the central nervous system (Dringen et al., 2016; McCann and Maguire-Zeiss, 2021; Ray et al., 2020; Sattar et al., 2016; Wisessaowapak et al., 2021).

Treatment of arsenic poisoning basically means the administration of *vicinal* dithiols (Bjørklund et al., 2020) such as the British Anti-Lewisite (BAL), 2,3-dimercaptopropane-1-ol, the archetype of arsenic antidotes. However, for BAL the disadvantages prevail: dreadful stench, low water solubility affording for a painful deep intramuscular injection as well as severe side-effects as it is toxic itself (Adams et al., 1990; Andersen, 1999). Hence, BAL was replaced by more water soluble and less toxic chelating agents such as sodium 2,3-dimercaptopropane-1-sulfonate (DMPS, unithiol) (Bjørklund et al., 2017; Lu et al., 2017; Nurchi et al., 2020; Petrunkin, 1956) or meso-2,3-dimercaptosuccinic acid (DMSA), the latter primarily developed for better antimony uptake in schistosomiasis treatment (Friedheim et al., 1954), and later also for heavy metal chelation (Liang et al., 1980). Their efficacy in heavy metal and metalloid detoxification has been widely proven and the underlying chemistry has been investigated (Aaseth et al., 2018; Andersen, 2004; Blanusa et al., 2005; Cavanillas et al., 2012; Gong et al., 2002; Guha Mazumder, 2003; Heinrich-Ramm et al., 2003; Kaviani et al., 2019; Suzuki et al., 2012).

As early as in the 1930s Cohen and co-workers (Cohen et al., 1931a, b, 1932a, b) conducted extensive studies regarding the chemistry and the concomitant therapeutic action of various arylarsenic compounds. They report that variation in the efficacy of pentavalent arsenicals is (in part) due to different rates of As(V) reduction. However, no straightforward correlation between redox potential and toxicity of the respective arsenicals could be found. Contributions by Cullen and co-workers regarding both arsenic in the environment (Cullen and Reimer, 1989) and mechanistic studies (Cullen et al., 1984a, b), the latter focusing on the reaction of methylarsenicals with various thiols, considerably improved the understanding of arsenic–thiol interactions. So far, the structure of (di)thiol conjugates of (substituted) phenylarsenicals have only scarcely been investigated by NMR and XRD, among them the unsubstituted, trivalent phenylarsine oxide (PAO) together with its interchangeably used dichloro analog (Aksnes and Bjørøy, 1975; O'Connor et al., 1989), and the *p*-APAA conjugate

of 6,8-dimercaptooctanoic acid (von Döllen and Strasdeit, 1998). Very recent work on the interaction of arsenous acid with BAL and the resulting products illustrate the ongoing interest in and importance of understanding the chemistry behind these detoxification processes (López-Moreno et al., 2018).

The related reaction of pentavalent phenylarsonic acids with (di)thiols is more complex as it is, in general, a two-stage process. Initially, the thiol is oxidized while the pentavalent arsenical is reduced to its trivalent analog and, subsequently, the latter is covalently bound to (remaining) thiol molecules (Cohen et al., 1931b; Cullen et al., 1984b; Kretzschmar et al., 2014). Serum and intracellular thiols such as the tripeptide glutathione (GSH) are the first target molecules for incorporated arsenicals (Delnomdedieu et al., 1993; Doerge et al., 2020) to react with *in vivo* and, hence, become reduced and conjugated. But for the success of the detoxification therapy the chelation by administered dithiols is crucial and therefore in this work the combination of redox and conjugation reactions between DMPS and pentavalent phenylarsenicals is investigated. For a better understanding of the thiol-arsenic reactions as well as structural impacts on reactivity and stability, we performed fundamental research focusing on the chelation agent DMPS and four phenylarsonic(V) acids, possessing different types and positions of polar substituents (Scheme 1), *i.e.*, phenylarsonic acid (PAA), 4-hydroxy-3-nitrophenylarsonic acid (HNPA), 2-aminophenylarsonic acid (*o*-APAA) and 4-aminophenylarsonic acid (*p*-APAA). This comprises the elucidation of both the solution and the crystal structures of trivalent conjugates formed by the reaction of *RS*-DMPS with the pentavalent organoarsenic compounds by one- and two-dimensional NMR spectroscopic methods and single-crystal X-ray diffraction. Furthermore, the dynamic behavior regarding the interconversion of the formed diastereomers, and the replacement of GSH by DMPS are investigated.

2. Materials and methods

2.1 Materials

Caution! The arsenic compounds used in this study are toxic and should be handled with care. All arsenic compounds used were of analytical grade and purchased from Acros Organics. Glutathione (>99%, Sigma-Aldrich) and *RS*-DMPS (95%, Alfa-Aesar) were used as obtained without further purification to prepare stock solutions in deuterium oxide (D₂O, 99.98%, Armar

Chemicals) for NMR experiments and in H₂O for single crystal preparation. For pH adjustment and pH dependent measurements, diluted deuteriochloric acid (DCl) made from concentrated DCl (35 wt.-% in D₂O, 99 atom-% D, Sigma-Aldrich) or diluted sodium deuterioxide (NaOD) made from concentrated NaOD (40 wt.-% in D₂O, 99 atom-% D, Sigma-Aldrich) in D₂O were added, respectively. The use of buffers was avoided; see considerations stated with Fig. S13).

2.2 Sample preparation for reaction monitoring

The samples were degassed to prevent autoxidation by dissolved oxygen and used immediately after preparation. Reaction samples were prepared by diluting appropriate volumes of stock solutions to obtain reaction mixtures of 5 mM arsenical(V) and 15 mM DMPS. pH was adjusted to 6.0 ± 0.5 with pH meter reading uncorrected for deuterium, and was stable within ± 0.2 units during the reaction. This pH was chosen according to species distribution calculations performed for mixtures of the arylarsenic compounds with GSH or DMPS (Figs. S14 and S15), showing that at $\text{pH } 6.0 \pm 0.5$ speciation undergoes only minor changes with pH.

2.3 NMR spectroscopy

All experiments were performed on a Bruker Avance III 500 spectrometer with a magnetic field of 11.75 T corresponding to resonance frequencies of 500.13 and 125.76 MHz for ¹H and ¹³C, respectively, using a 5 mm direct detection probe with z-gradient. For structure elucidation, 2D-NMR, *i.e.* H,H-COSY, H,H-NOESY, H,C-HSQC and H,C-HMBC spectra were recorded. All spectra were referenced relative to 3-(trimethylsilyl)-propionic acid sodium salt (TSP, 98%, Sigma-Aldrich) with $\delta_{\text{H}} = 0$ ppm and $\delta_{\text{C}} = 0$ ppm. All measurements were carried out at $(22 \pm 0.1) ^\circ\text{C}$ and in particular cases additionally at $5 ^\circ\text{C}$ to reduce the reaction rate, with temperature stability achieved by the spectrometer's temperature control combined with a BCU05 cooling unit (Bruker).

NMR signal assignment was carried out by means of H,H- and H,C-correlation spectra (*cf.* Supporting Information), scalar H,H coupling constants (*vide supra*) as well as integration of ¹H signal areas in order to discriminate the *syn* and the *anti* products' signals.

2.3 X-ray crystallography

In order to obtain single-crystals, aqueous solutions containing 20 mM of the phenylarsenic(V) acids and 80 mM of DMPS were allowed to react at room temperature in a desiccator over silica gel.

Crystals suitable for X-ray diffraction were selected under a microscope with polarized light and mounted on a glass capillary with a thin film of silicon grease. The data sets were collected on a IPDS-2T diffractometer (Stoe) using Mo K α radiation ($\lambda = 0.71073 \text{ \AA}$) at 150 K. The structures were solved by direct methods with SHELXS and all non-hydrogen atoms were anisotropically refined in full-matrix least-squares cycles against $|F^2|$ with SHELXL-2018/3 (Sheldrick, 2008; Sheldrick). Carbon-bound hydrogen atoms were placed in idealized positions and refined isotropically. In particular cases, *i.e.*, NH groups, the hydrogen coordinates were obtained directly from differential-Fourier-syntheses. Graphics of the molecular structures were generated with ORTEP32 (Farrugia, 1997) and POV-RAY (Persistence of Vision Pty. Ltd. Persistence of Vision Raytracer (Version 3.6). Retrieved from <http://www.povray.org/download/>, 2004).

Crystallographic data for the structures reported in this paper have been deposited with the Cambridge Crystallographic Data Centre under CCDC numbers 1019299, 1019300, and 1019298 for PAA–DMPS, HNPAA–DMPS, and *p*-APAA–DMPS, respectively. Copies of the data can be obtained free of charge on application to CCDC, 12 Union Road, Cambridge, CB2 1EZ, UK (Fax: + 44 1223 336033; e-mail: deposit@ccdc.cam.ac.uk).

2.4 Elemental analyses

For the elemental analyses the obtained crystalline products were used and carried out with a Vario Micro Cube analyzer (Elementar, Hanau, Germany).

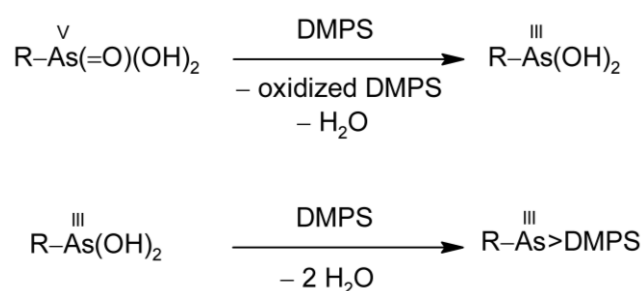
2.5 Redox potentials

Aqueous solutions of the reactants without further pH-adjustment were used to determine half-cell potentials by means of high ohmic multimeter reading of the potential difference between two chambers, one containing 5 mM arsenical(V) and 15 mM together with a Pt working electrode, and the other containing a saturated KCl solution together with a Ag/AgCl electrode as reference, both connected by a glass tube salt bridge filled with 1 M NH₄NO₃ solution.

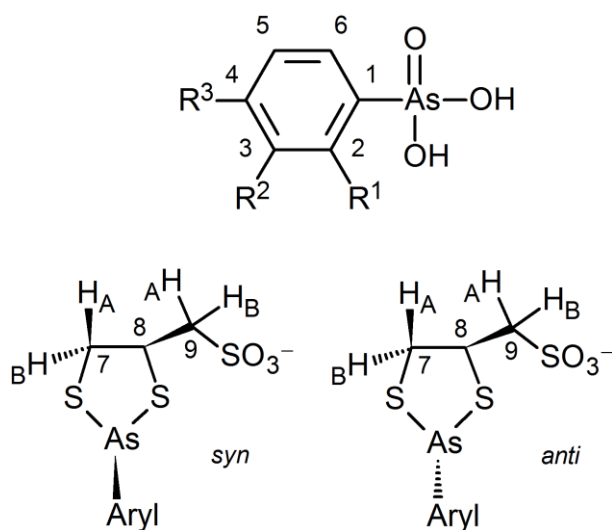
3. Results and Discussion

For all investigated phenylarsonic(V) acids the formation of trivalent phenylarsenic–DMPS conjugates, comprising five-membered chelate rings, alongside with oxidized DMPS di- and oligomers were obtained (Scheme 1). Since the chelating agent DMPS was used in its racemic

form, formation of product compounds with four different configurations is expected, that is (*R,R*) and (*S,S*) as well as (*R,S*) and (*S,R*) isomers. The trivalent arsenic atom and one DMPS carbon (C8 in Scheme 2) are chiral, resulting in two diastereomeric pairs of enantiomers (Fig. S1). For simplicity, in the following the isomers will be denoted as the *syn* and the *anti* products (Scheme 2), as we do not differentiate between their enantiomers. These terms (*syn* and *anti*) consider the orientation of the arsenic bound aryl residue relative to the DMPS CH₂-SO₃⁻ residue within the conjugate.



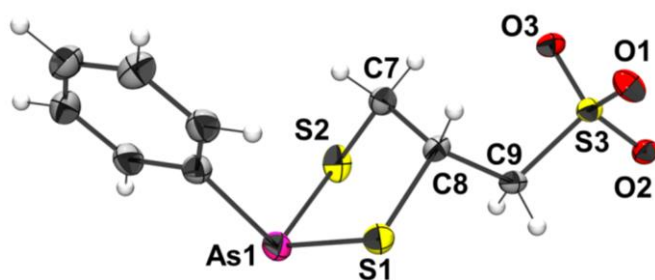
Scheme 1. Schematic reaction of pentavalent phenylarsonic acids with DMPS: redox reaction (upper trace) and conjugation (lower trace); R denoting (substituted) phenyl residues.



Scheme 2. Generic structures and labeling of the investigated pentavalent phenylarsonic acids (top) and the stereoisomers of their trivalent DMPS conjugates (bottom). R¹, R², R³ = H: phenylarsonic acid (PAA); R¹ = NH₂, R², R³ = H: 2-aminophenylarsonic acid (*o*-APAA); R¹, R² = H, R³ = NH₂: 4-aminophenylarsonic acid (*p*-APAA); R¹ = H, R² = NO₂, R³ = OH: 4-hydroxy-3-nitrophenylarsonic acid (HNPPAA); A and B denoting diastereotopic H atoms.

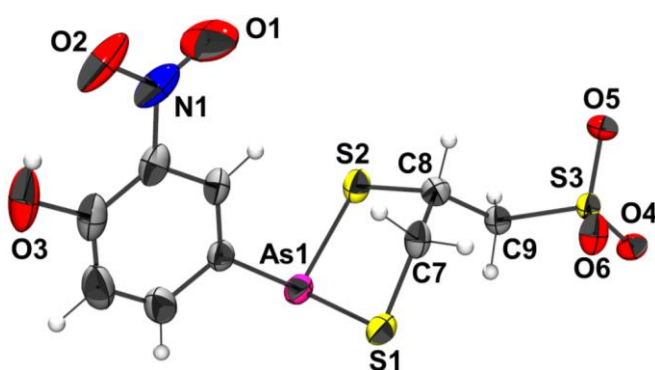
3.1 Crystal structures of phenylarsenic(III)–DMPS conjugates

In the course of our study we succeeded in growing crystals of the DMPS conjugates of three phenylarsenicals out of the four under investigation. Crystallographic parameters of data collection and structure refinement for the crystal structures of conjugates of DMPS with PAA, HNPA, and *p*-APAA are summarized in Table S1. Whereas the arsadithiolanes obtained from PAA (Fig. 1) and from HNPA (Fig. 2) crystallized as sodium salts, the corresponding product obtained from *p*-APAA (Fig. 3) crystallized as a zwitterionic compound with the protonated *p*-amino group serving as the cationic component. In contrast to the DMPS conjugates obtained from PAA and HNPA, which crystallize as the *anti* isomers in high purity (which will be made use of for purification of the *anti* isomer and its utilization in isomerization studies, *vide infra*), the product obtained from *p*-APAA crystallized as a mixture of enantiomers of the *anti* product and an enantiomer of the *syn* product on the same site of the asymmetric unit in a disordered manner. As the HNPA–DMPS conjugate also exhibits disorders in the solid state structure (in this case the phenyl groups are disordered), only one of the three crystal structures is basically free of severe disorders, and therefore we cannot discuss substituent effects on bond lengths in a comparative way. A structural feature of greater importance for the further discussion, *i.e.* characterization in solution and the effects of $^3J(\text{H,H})$ coupling, however, can be extracted even from the disordered structures. That is, the H-C(8)-C(7)-H torsion angles of the *anti* products were found in the range 61–71° (for the *exo* H atom at C7) and 47–58° (for the *endo* H atom at C7). In the *syn* product, which is contained in the structure of the *p*-APAA–DMPS conjugate (Fig. 3, bottom) there is a significantly larger difference between the torsion angles, *i.e.*, 179° for the *endo* H atom at C7 and 58° for the *exo* H atom. Even though the hydrogen atoms in the crystal structures had been placed in idealized positions, the H-C-C-H torsion angles should be representative of notable differences between the *anti* and *syn* isomers. Although two out of the three crystal structures suffer disorder effects, it appears that for all conjugates the two As–S bonds within one molecule show systematically different bond lengths. In fact, the bonds between the arsenic and that sulfur adjacent to the chiral carbon atom are shorter by ca. 0.01–0.03 Å. This is similar to the situation in the lipoic acid conjugate of PAO (0.03 Å)³⁵ but in contrast to the BAL adduct of tolyldichloroarsine with the latter bond being longer by 0.05 Å (Adams et al., 1990).



228

229 **Fig. 1.** Molecular structure of the anion of the PAA-DMPS conjugate sodium salt $\text{Na}_2(\text{PAA-DMPS})_2(\text{H}_2\text{O})_3$ in the crystal (one of the two crystallographically independent anions is shown,
230
231 ellipsoids set at 50% probability).



232

233 **Fig. 2.** Molecular structure of the anion of the HNPA-DMPS conjugate sodium salt
234 $\text{Na}_2(\text{HNPA-DMPS})_2(\text{H}_2\text{O})_3$ in the crystal (one of the two crystallographically independent
235 anions is shown, ellipsoids set at 50% probability).

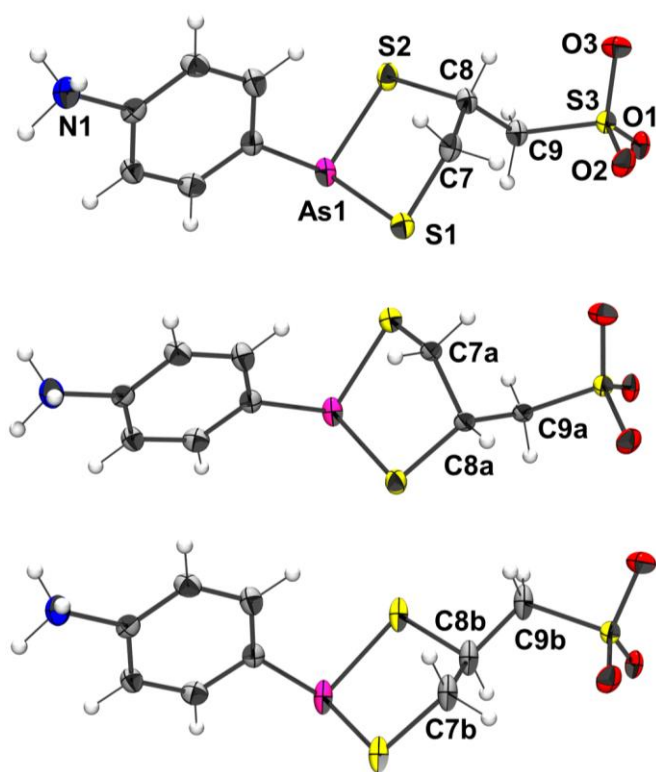


Fig. 3. Molecular structure of the *p*-APAA–DMPS conjugate in the crystal (ellipsoids set at 50% probability). Two enantiomers of the *anti*-product (top and middle) and one enantiomer of the *syn*-product (bottom) occupy the same site in approximate ratio 8:1:1. Whereas the position of the aryl group is identical for the three isomers, the arsacyclic part of the molecules (incl. the sulfonate group) occupies alternative positions.

3.2 Solution structures of phenylarsenic(III)–DMPS conjugates

Comprehensive ^1H and ^{13}C NMR data of the obtained conjugates as well as representative two-dimensional NMR spectra is given as Supplementary material. Coupling constants (J) and chemical shifts (δ) can be used to assign the stereoisomers as follows.

The protons of the arsadithiolane ring of the *syn* products are, in general, more shielded (show smaller δ) than the corresponding protons in the *anti* products. Particularly H7A and H8 in the *o*-APAA–DMPS *syn* conjugate are shielded by 0.14 and 0.31 ppm, respectively. This can be attributed to an increased steric demand in the *syn* configuration. Since the C7 methylene group is structurally fixed in the five-membered ring, owing to their diastereotopicity the protons in both the *anti* and *syn* product show *geminal* coupling constants $^2J(7A,7B)$ of ≈ 13 Hz, and significant δ_{H} differences.

The C9 methylene protons in the *syn* products are virtually equivalent, with the same δ_{H} and no 2J observable. The *vicinal* coupling constants (3J) show values of ≈ 6.7 Hz, which is comparable to averaged values in alkyl chains. In the *anti* products $^2J(\text{H9A,B})$ were determined to be 14.4 Hz. According to the Karplus relationship (Karplus, 1963), with $^3J(\text{H8,H9A})$ and $^3J(\text{H8,H9B})$ being 8.3 and 5.3 Hz, the couplings exhibit an angle-dependence attributed to *trans* and *gauche* patterns, respectively, suggesting a reduced flexibility of the $\text{CH}_2\text{-SO}_3^-$ residue (rotation about the C8–C9 axis is slow on the NMR time scale).

Whereas $^3J(\text{H8,H7A})$ and $^3J(\text{H8,H7B})$ in the *anti* products are equal (HNPAAs: 4.1 Hz, *p*-APAA: 4.4 Hz) or at least very similar (*o*-APAA: 4.3 and 3.8 Hz), the *syn* products exhibit remarkable differences (9.2 vs. 3.9, 9.0 vs. 3.9, and 9.7 vs. 4.1 Hz for HNPAAs, *p*-APAA, and *o*-APAA, respectively). This is in total agreement with observations in the crystal structures (*vide supra*). They reveal only small differences in the torsion angles between H8 and the *endo* and *exo* H7 for the *anti* products (corresponding to similar 3J), but reveal large differences and thus varying 3J values in the *syn* products. Consequently, H7A can be denoted as the *endo* and H7B as the *exo* hydrogen. This assignment is corroborated by NOESY (Fig. S6), showing dipolar interaction between H2 (*ortho*) and H7A but not H7B.

For the trivalent arsenic–DMPS conjugates the ^{13}C NMR signals are shifted downfield (larger δ_{C}) by about 1.3 ppm (C9), 1.5 ppm (C8), and 1.1 ppm (C7) compared to free DMPS. The most profound structural and hence spectral changes occur at the asymmetric carbon, C8 and, to some extent, for those in their direct vicinity. $\Delta\delta_{\text{C}}$ between *syn* and *anti* products are -0.97 , -0.93 , and -0.85 ppm (C9), 2.21, 2.19, and 2.07 ppm (C8), and 0.40, 0.39, and 0.28 ppm (C7) for the conjugates of HNPAAs, *o*-APAA, and *p*-APAA, respectively. Even the aryl carbons are sensitive to configuration. Significant $\Delta\delta_{\text{C}}$ can be found in the HNPAAs conjugate for C3 (0.63 ppm), in the *p*-APAA conjugate for C2 (-0.84 ppm) and C3 (0.35 ppm) as well as in the *o*-APAA conjugate for C1 (0.58 ppm) and C6 (0.18 ppm).

3.3 Monitoring the phenylarsenic(V)–DMPS reaction

By simply mixing aqueous solutions of both DMPS and phenylarsonic(V) acids at room temperature the reaction starts instantly.

The reaction progress is slow enough to be monitored by ^1H NMR at room temperature. Fig. 4 shows exemplary time-dependent spectra of DMPS systems of HNPAAs as well as *o*- and *p*-APAA. In the course of the reaction the pentavalent arsenicals' signals (indicated by

asterisks) decrease while the two sets of signals for the *syn* and *anti* isomers appear and increase. According to the reaction of pentavalent methyl- and arylarsenic compounds as well as inorganic arsenate with several other thiols (Cullen et al., 1984b; Delnomdedieu et al., 1993; Kretzschmar et al., 2014) the reaction occurs *via* two reaction steps: (1) redox reaction with oxidation of DMPS and concomitant reduction of the pentavalent arylarsenic acid to its trivalent analog (arylsenite), and (2) the subsequent chelation of the latter by further (free) DMPS, *cf.* Scheme 1. Since the trivalent analog R–As(OH)₂ cannot be observed by ¹H NMR (Cullen et al., 1984a; Kretzschmar et al., 2014), the second reaction step is considered to be significantly faster and the redox reaction to be rate determining. For further information on the nature of the oxidized DMPS see Fig. S7 and Scheme S2.

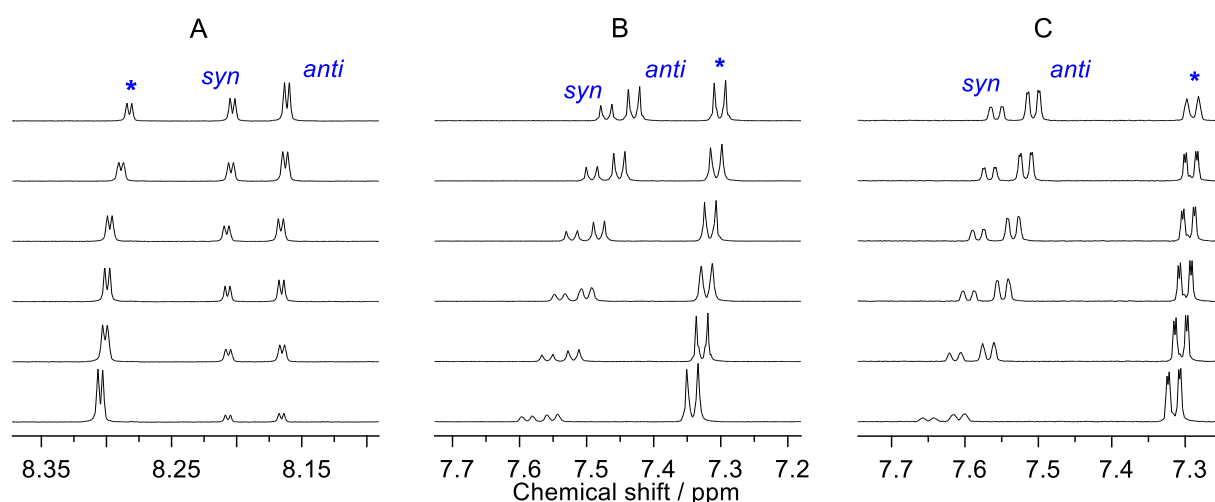


Fig. 4. Section of the aromatic *ortho* ¹H signals of time-dependent ¹H NMR spectra for DMPS systems of HNPA (A), *p*-APAA (B), and *o*-APAA (C). Signals of the formed trivalent diastereomeric conjugates are denoted *syn* and *anti*, and those of the pentavalent precursors are indicated by asterisks. From bottom to top: 15, 30, 45, 60, 90, and 120 min after mixing. Signals of the aliphatic protons are shown in Figs. S8–S11.

As already observed by Cullen et al. (1984b) for the reaction of trimethylarsine with mercaptoethanol, but in contrast to our own results (Kretzschmar et al., 2014) for the reaction of pentavalent phenylarsenic compounds with GSH, the obtained curves did not fit any simple rate expression. This is likely due to the variety of possible di- and oligomeric oxidation products of DMPS (Fig. S7 and Scheme S2) involved in the reaction equilibrium. In order to evaluate the reaction progress and allowing for comparison between the systems, the half-lives (*t*_{1/2}),

indicating that point of time when 50% of the initial As(V) is converted to As(III), were determined. Therefore, in the time-dependent spectra (Fig. 4) the phenyl signals of both the As(V) reactant and the As(III) conjugate were integrated and the obtained molar fractions plotted *versus* time, giving $t_{1/2}$ as the intercept of both curves (Scheme S1).

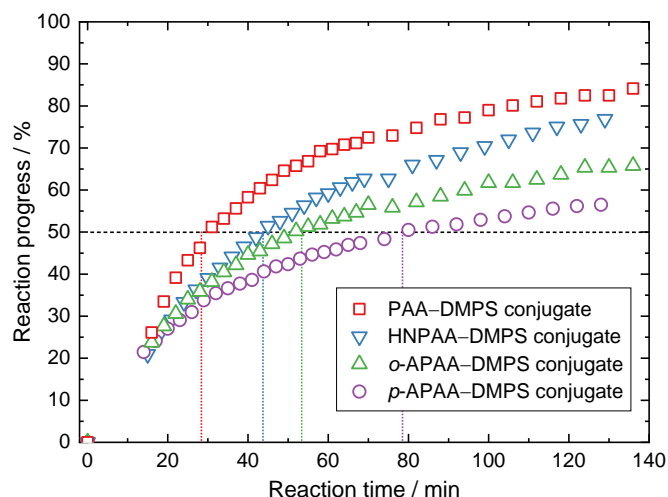


Fig. 5. Time-dependent formation of As(III)-DMPS conjugates of different phenylarsonic(V) acids for pH 6 solutions initially 5 mM in the arsenic(V) component and 15 mM in DPMS at 5 °C. The reaction progress is expressed in terms of reacted arsenic(V) starting material as determined from mole fractions obtained from NMR signal integration. Colored dotted lines indicate the respective half-lives.

For a convenient and reliable observation of the reaction progress, the sample series were measured at 3 : 1 molar ratio (DMPS : As) and at 5 °C, see Figs. 5 and S16. The obtained $t_{1/2}$ values are 29, 43, 53, and 79 minutes for PAA, HNPAA, *o*-APAA, and *p*-APAA, respectively, at pH = 6 ± 0.5. The relative order of $t_{1/2}$ values of the DMPS reactions is similar to that of kinetic investigations of these arylarsenicals with GSH (Kretzschmar et al., 2014). In principle, at comparable conditions the reaction of phenylarsonic(V) acids is considerably faster with DMPS than with GSH, with $t_{1/2}$ values being 2-3 times shorter than for the GSH reactions.

Although not investigated in detail the reaction monitoring at different pH showed that in solutions of DMPS and HNPAA at pH 1, the latter is quantitatively converted within 90 minutes, whereas at pH 10 no reaction can be observed even after 8 days. According to the pK_a values of the reactants (Arnold et al., 1985; Huckerby et al., 1985; Nualláin and Cinnéide, 1973; Roerdink and Aldstadt, 2005) (*cf.* Tables S2–S3 and Figs. S14–S15), the reaction kinetics are mainly attributed to the arsenicals' speciation. The amino derivatives (*o*- and *p*- APAA) are

able to form cations at very low pH by protonation of the amino group. At $1 < \text{pH} \leq 3.5$ –4 (depending on the individual arsenical), but prior to the deprotonation of the As-bound OH groups, the latter exist as neutral molecules. Upon increasing the pH, in general at the latest at pH 4.5, only negatively charged arsenic(V) species exist. Owing to the deprotonation of the SO_3H group, DMPS is considered to be negatively charged even at low pH values. Deprotonation of the SH groups starts above pH 8. Consequently, the lower the pH, the faster the reaction, since the total number of negative charges and, hence, repulsion is decreased. A similar behavior and interpretation was recently reported for the reaction of arsenite and methylarsenicals with GSH by Doerge et al. (2020) and, earlier, it was already suggested for the reaction of methylarsenicals with (di)thiols that the reaction involves the unionized thiol group (Cullen et al., 1984a, b). Accordingly, the pH-dependent rate differences are primarily impacted by speciation of the arsenicals.

Additionally, the relative order of the reaction rates is apparently influenced by the half-cell potentials of the reactants (Table S4). It has to be considered that these potentials are also pH-dependent. Although the reduction ability of DMPS increases with increasing pH, the speciation (anionic nature of both reactants) hampers the interaction due to electrostatic repulsion at higher pH values.

3.4 Interconversion between *anti* and *syn* isomer

Considering the *anti* : *syn* ratio, literature reveals a dependence on the nature of the chelator only (Aksnes and Holak, 1982; Dill et al., 1987; Dill et al., 1991; O'Connor et al., 1989). For the reaction of DMPS with both the *trans*-2-chlorovinylarsine oxide (Lewisite oxide) and phenyldichloroarsine (PDA, trivalent analog of PAA) O'Connor et al. (1989) found an *anti* : *syn* ratio of 2.0 whereas the reaction with BAL (OH instead of the SO_3^- group) yields a ratio ≥ 4 , whereupon they state that the organic group on the arsenical does not appear to affect the ratio appreciably.

In the systems investigated here it appeared that the *anti* : *syn* ratio depends on both the reaction time and the nature of the arsenic-bound aryl residue. The *anti* : *syn* ratio increases with time for PAA, HNPA, and *p*-APAA up to an equilibrium value of 2.0 ± 0.1 , whereas in the case of *o*-APAA the *anti* : *syn* ratio amounts ≈ 2.2 already at the beginning and decreases slightly with time (Fig. 5). Dill et al. (1991) investigated the dynamics of the adduct yielded by the reaction of PDA with 1,2-dithiopropene (PDT, forming an analogous five-membered ar-

sadithiolane ring with a methyl group instead of the methylenesulfonate as in DMPS) and determined the temperature-dependent rates of interconversion between the isomers. Accordingly, by increasing the temperature from 288 to 310 K the *anti*→*syn* conversion, k_1 , and the *syn*→*anti* conversion, k_2 , increase from 0.55 to 2.93 and from 1.30 to 6.68 1/s, respectively, corresponding to very similar activation energies of 57.2 and 55.9 kJ/mol, respectively. Additionally, they found the conversion rate to be dependent on the adduct concentration, but not on that of the ligand though ascribing the interconversion to a ligand exchange reaction.

As seen from the presented NMR spectra, and qualitatively shown by exchange spectroscopy (EXSY, Fig. S12) the interconversion rate is slow on the NMR time scale, hence allowing for the observation of two sets of well-resolved signals, one for each isomer, which is in full agreement with the small k values reported by Dill et al. (1991). Regarding their PDA–PDT adduct, calculation of the $k_2 : k_1$ ratio yields 2.3 which is equal to the *anti* : *syn* ratio, since $k_2 : k_1$ is not determined by the magnitude of the activation energies (of either conversion step) but their difference, ΔE_a . The *anti* : *syn* ratios obtained in our experiments suggest ΔE_a values of ≈ 1 kJ/mol, thus being very similar to ΔE_a of 1.3 kJ/mol found by Dill et al. (1991). Furthermore, for the interconversion between the PDA–1,3-dimercaptopropane-2-ol adduct isomers (forming a six-membered ring) the activation energies of 42.9 and 37 kJ/mol yield ΔE_a of 5.9 kJ/mol, corresponding to $k_2 : k_1 = 4$ equivalent to an *anti* : *syn* ratio of 4 (Dill et al., 1991).

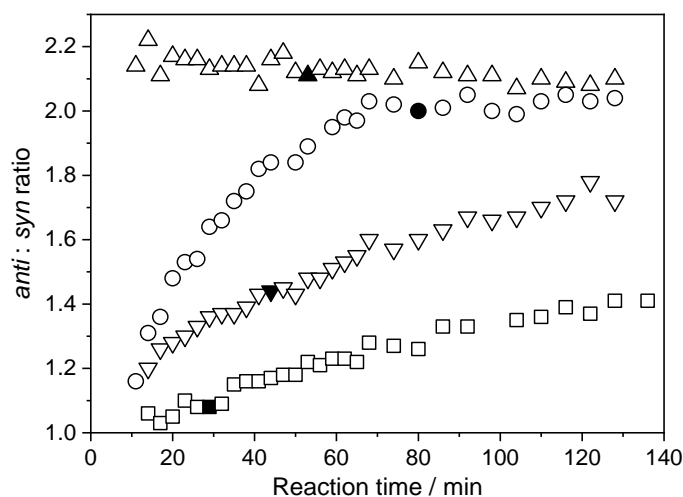


Fig. 6. Time-dependent *anti* : *syn* ratios of DMPS conjugates of PAA (\square), HNPA (∇), *p*-APAA (\circ), and *o*-APAA (\triangle). Filled symbols indicate $t_{1/2}$.

At the beginning, the redox reaction determines the overall reaction behavior. Once reduced, for the reaction (conjugation) of racemic DMPS and (prochiral) As(III) the sterics impact the

kinetics of the diastereomer formation, favoring the *anti* product after equilibration. As can be derived from Fig. 6, two different types of rate constants have to be considered – one for the conjugate formation and one for the interconversion. Each type exhibits individual rates for either diastereomer, whereas the former are, in principle, higher than the latter. Consequently, the *ortho*-position of the amino group in *o*-APAA impacts the isomeric ratio already during the conjugate formation, being attributed to a strong steric influence of the amino group. It can be further concluded that the energy barriers for the interconversion are high, since no significant ratio changes occur. In the case of PAA, with the smallest steric hindrance, the ratio increases slowly with time, indicating only narrow differences in the energy barriers with the equilibrium being more depending on the interconversion rate rather than individual formation rates.

In contrast to the observations of Dill *et al.* we found a strong dependence of the ligand concentration on the interconversion rates. Moreover, by re-dissolution of a single-crystal containing the *anti* isomer only, Fig. 7, even 10 days later we found the *syn* isomer to be less than 7 % of the total amount of conjugate, implying a very small interconversion rate. However, 12 hours after addition of two equivalents of free DMPS to this solution we observed the usual *anti* : *syn* ratio of 2.0 ± 0.1 . We therefore conclude that free DMPS accelerates remarkably the interconversion of the *anti* and *syn* products, according to a bimolecular reaction (*cf.* Scheme S3).

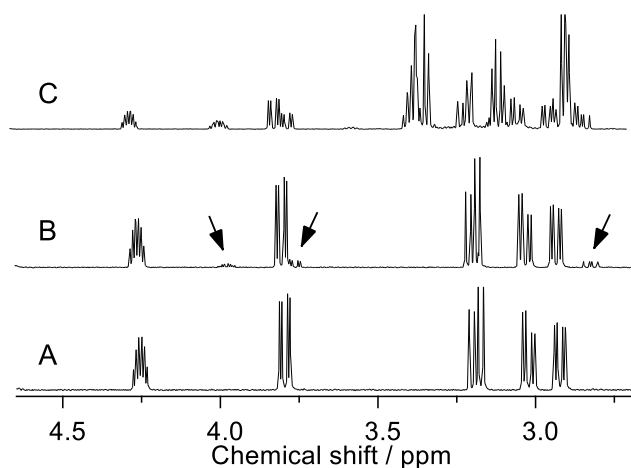


Fig. 7. Aliphatic region of ^1H NMR spectra of a single-crystal obtained from the reaction of PAA with DMPS immediately (A) and 10 days (B) after re-dissolution in D_2O , and 12 hours after addition of two equivalents of DMPS (C). The arrows indicate the appearing signals as compared to the bottom trace.

3.5 Replacement of the monothiol GSH by chelating dithiol DMPS

Since GSH is an important intracellular reducing and detoxification agent for heavy metals and metalloids, it is likely that, *e.g.*, incorporated arsenic is bound primarily to GSH. Addition of DMPS to a solution containing the conjugate of, for instance, HNPAA and GSH, revealed an instant replacement of the monothiol from the trivalent arsenic and a quantitative chelation of the latter by DMPS (see Fig. S17 for ^1H spectra and generic structures). Similar behavior has been observed by Delnomdedieu et al. (1993) for arsenate (AsO_4^{3-}). Both the yield and the rate of this reaction are remarkable, the former being attributed to the stability of these compounds, and the latter confirming the redox reaction (upper trace in Scheme 1) to be rate determining. Since HNPAA was already reduced (and conjugated) by GSH to an arsenic(III) compound, DMPS does not need to undergo the significantly slower redox reaction, but is able to act instantaneously as the chelator. Promptly after the admixture of DMPS the *anti* : *syn* ratio is 1 : 1, whereas 12 hours after addition of free DMPS an *anti* : *syn* ratio of 2 : 1 was observed. These results are comparable to those of the reaction monitoring. Prior to the *anti*–*syn* interconversion, the 1 : 1 ratio of these isomers is due to the use of racemic DMPS with equal probability of the formation of either isomer. Subsequently, with increasing time, interconversion proceeds and converges to the usual ratio favoring the *anti* isomer.

4. Conclusion

By means of both the ^1H NMR signals of oxidized DMPS and the trigonal pyramidal coordination geometry of the conjugates' arsenic atom in the crystal structures, it can be unambiguously proven that DMPS reduces the studied arsenic(V) compounds to their arsenic(III) analogs in addition to the conjugation as bidentate chelating agent. Particularly the dependence of the *vicinal* coupling constant on the torsion angle allows a good perception of the solution structures which enables the assignment of the products and the comparability with the solid structures.

Among the investigated phenylarsonic acids, the presence and nature of the substituents, including OH, NO_2 , and NH_2 (in *ortho* or *para* position) impacts not only the arrangement within the crystalline products but in particular the reaction behavior. The latter is illustrated by the

similar succession of $t_{1/2}$ values for GSH (Kretzschmar et al., 2014) and DMPS conjugate formation depending on the individual phenyl residues. Analogous to the correlation between toxicity of organoarsenic(V) compounds and reaction rate for their GSH conjugation – the latter occurring *in vivo* for arsenic detoxification –, the reaction of DMPS again is fastest for the most toxic among the phenylarsonic(V) acids studied. Based on comparison of determined half-lives and velocities, the overall reaction rates further depend (beside temperature and concentration) on pH, the latter influencing both the reduction potentials and the speciation of the reactants. Since electrostatic repulsion between the reactants is able to prevent the reaction, the pH-dependent speciation has to be considered as a prerequisite to initiate the reaction, together with sufficient differences in the redox potentials. Protonated thiol groups are favorable for the reaction progress and because they are stable beyond the physiological pH for DMPS this underlines its relevance for detoxification.

As for other As(V)–thiol systems, the redox reaction is the rate determining step. Significantly faster is the promptly occurring chelation step once the arsenic is reduced to its trivalent form. This could be proven additionally by the immediate replacement of the intracellular tripeptide GSH bound to arsenic, emphasizing the suitability of DMPS in arsenic detoxification. Conjugates of DMPS derivatives are thus much more stable than those of GSH, which is supported by the 2-3 times smaller magnitude of $t_{1/2}$ values for the reaction of DMPS with arylarsenic(V) compounds compared to GSH. The ability to reduce As(V) together with the fast reaction as well as the high stability of the yielded products gives a better understanding why the use of DMPS is conceivable in arsenic detoxification and for replacement, but also for the protection of thiol containing molecules, beyond biological relevance.

Although the *anti* : *syn* ratio of the isomers formed is mainly influenced by the dithiol rather than the aryl residue, showing values of 2.0 ± 0.1 in equilibrium, the sterics exert influence on the ratio particularly at the beginning of the reaction progress. The difference in energy barriers for the conversion of the isomers was estimated to be less than 2 kJ/mol, whereas the energy barriers themselves are assumed to be in the order of 60 kJ/mol. Furthermore, the interconversion is dependent on the concentration of free ligand, implying a bimolecular mechanism. Together with the solutions' isomeric ratio, the crystal structures reveal that the *anti* isomer crystallises preferably, either due to higher solubility of the *syn* isomer or as a result of preferred seed crystal formation of the *anti* isomer (which is present in higher concentration) and continuous transformation of *syn* into *anti* isomer in the course of crystallization.

Declaration of Competing Interest

485 The authors report no declarations of interest.

486 **Appendix A. Supplementary data**

487 Supplementary material related to this article (Generic stereostructures; comprehensive NMR
488 spectroscopic characterization of the compounds investigated, crystallographic information
489 files (cif); NMR spectra showing the replacement of GSH from its roxarsone conjugate by
490 DMPS; schemes visualizing the half-life determination, and the bimolecular reaction of
491 *syn/anti* interconversion; pK_a values of the arsenicals investigated; half-cell potentials of the
492 reactants; species distribution calculations) can be found, in the online version, at doi:
493 <https://doi.org...>

494 **CRedit authorship contribution statement**

495 The manuscript was written through contributions of all authors. All authors have given ap-
496 proval to the final version of the manuscript.

497 **Acknowledgement**

498 We thank Regina Hüttel, Institute of Physical Chemistry, TU Bergakademie Freiberg, for her
499 support with the redox potential measurements, Philipp Rath sack and Klara Sander, Institute
500 of Analytical Chemistry, TU Bergakademie Freiberg, for performing the species distribution
501 calculations and for the support in the literature search, respectively.

502

503 **References**

- 504 Aaseth, J., Ajsuvakova, O.P., Skalny, A.V., Skalnaya, M.G., Tinkov, A.A., 2018. Chelator
505 combination as therapeutic strategy in mercury and lead poisonings. *Coord. Chem. Rev.* 358,
506 1-12. <https://doi.org/10.1016/j.ccr.2017.12.011>.
- 507 Adams, E., Jeter, D., Cordes, A.W., Kolis, J.W., 1990. Chemistry of organometalloid
508 complexes with potential antidotes: structure of an organoarsenic(III) dithiolate ring. *Inorg.*
509 *Chem.* 29, 1500-1503. <http://dx.doi.org/10.1021/ic00333a012>.
- 510 Aksnes, D.W., Bjorøy, M., 1975. NMR Studies on Cyclic Arsenites. 1H NMR Spectral
511 Analysis and Conformational Studies of 2-Chloro-5-methyl- and 2-Phenyl-5-methyl-1,3,2-
512 oxathiarsolane and 2-Chloro-5-methyl-1,3,2-dithiarsolane and -1,3,2-dioxarsolane. *Acta*
513 *Chem. Scand. A* 29, 672-676.

514 Aksnes, D.W., Holak, T.A., 1982. Spectral analysis of the high-resolution proton-coupled
 515 carbon-13 NMR spectra of 1,3,2-dithiarsolanes. *Org. Magn. Res.* 18, 28-32.
 516 <http://dx.doi.org/10.1002/mrc.1270180107>.

517 Andersen, O., 1999. Principles and Recent Developments in Chelation Treatment of Metal
 518 Intoxication. *Chem. Rev.* 99, 2683-2710. <http://dx.doi.org/10.1021/cr980453a>.

519 Andersen, O., 2004. Chemical and Biological Considerations in the Treatment of Metal
 520 Intoxications by Chelating Agents. *Mini-Rev. Med. Chem.* 4, 11-21.
 521 <http://dx.doi.org/10.2174/1389557043487583>.

522 Anderson, C., 1983. Arsenicals as feed additives for poultry and swine., in: Lederer, W.H.,
 523 Fensterheim, R.J. (Eds.), *Arsenic: Industrial, Biomedical, Environmental Perspectives*. Van
 524 Nostrand Reinhold, New York, pp. 89-99.

525 Arnold, A.P., Canty, A.J., Reid, R.S., Rabenstein, D.L., 1985. Nuclear magnetic resonance
 526 and potentiometric studies of the complexation of methylmercury(II) by dithiols. *Can. J.*
 527 *Chem.* 63, 2430-2436. <http://dx.doi.org/10.1139/v85-402>.

528 Bjørklund, G., Mutter, J., Aaseth, J., 2017. Metal chelators and neurotoxicity: lead, mercury,
 529 and arsenic. *Arch. Toxicol.* 91, 3787-3797.

530 Bjørklund, G., Oliinyk, P., Lysiuk, R., Rahaman, M.S., Antonyak, H., Lozynska, I., Lenchyk,
 531 L., Peana, M., 2020. Arsenic intoxication: general aspects and chelating agents. *Arch.*
 532 *Toxicol.* 94, 1879-1897.

533 Blanusa, M., Varnai, V.M., Piasek, M., Kostial, K., 2005. Chelators as Antidotes of Metal
 534 Toxicity: Therapeutic and Experimental Aspects. *Curr. Med. Chem.* 12, 2771-2794.
 535 <http://dx.doi.org/10.2174/092986705774462987>.

536 Cavanillas, S., Chekmeneva, E., Ariño, C., Díaz-Cruz, J.M., Esteban, M., 2012.
 537 Electroanalytical and isothermal calorimetric study of As(III) complexation by the metal
 538 poisoning remediators, 2,3-dimercapto-1-propanesulfonate and meso-2,3-dimercaptosuccinic
 539 acid. *Anal. Chim. Acta* 746, 47-52. <http://dx.doi.org/10.1016/j.aca.2012.08.005>.

540 Chauhan, S., Chauhan, S., D'Cruz, R., Faruqi, S., Singh, K.K., Varma, S., Singh, M.,
 541 Karthik, V., 2008. Chemical warfare agents. *Environ. Toxicol. Pharmacol.* 26, 113-122.
 542 <https://doi.org/10.1016/j.etap.2008.03.003>.

543 Chen, B., Liu, Q., Popowich, A., Shen, S., Yan, X., Zhang, Q., Li, X.-F., Weinfeld, M.,
 544 Cullen, W.R., Le, X.C., 2015. Therapeutic and analytical applications of arsenic binding to
 545 proteins. *Metallomics* 7, 39-55. <http://dx.doi.org/10.1039/C4MT00222A>.

546 Cohen, A., King, H., Strangeways, W.I., 1931a. CCCCL.-Trypanocidal action and chemical
 547 constitution. Part XI. Aromatic arsonic acids containing amide groups. *J. Chem. Soc.*, 3236-
 548 3257. <http://dx.doi.org/10.1039/JR9310003236>.

549 Cohen, A., King, H., Strangeways, W.I., 1931b. CCCCXXI.-Trypanocidal action and
 550 chemical constitution. Part X. Arylthioarsinites. *J. Chem. Soc.*, 3043-3057.
 551 <http://dx.doi.org/10.1039/JR9310003043>.

552 Cohen, A., King, H., Strangeways, W.I., 1932a. 371. Trypanocidal action and chemical
553 constitution. Part XIII. Arylthioarsinites from cysteine and glutathione. J. Chem. Soc., 2505-
554 2510. <http://dx.doi.org/10.1039/JR9320002505>.

555 Cohen, A., King, H., Strangeways, W.I., 1932b. 435. Trypanocidal action and chemical
556 constitution. Part XIV. The relative velocity of oxidation of arylarsenoxides. J. Chem. Soc.,
557 2866-2872. <http://dx.doi.org/10.1039/JR9320002866>.

558 Cullen, W.R., McBride, B.C., Reglinski, J., 1984a. The reaction of methylarsenicals with
559 thiols: Some biological implications. J. Inorg. Bioch. 21, 179-193.
560 [http://dx.doi.org/10.1016/0162-0134\(84\)83002-0](http://dx.doi.org/10.1016/0162-0134(84)83002-0).

561 Cullen, W.R., McBride, B.C., Reglinski, J., 1984b. The reduction of trimethylarsine oxide to
562 trimethylarsine by thiols: a mechanistic model for the biological reduction of arsenicals. J.
563 Inorg. Biochem. 21, 45-60. [http://dx.doi.org/10.1016/0162-0134\(84\)85038-2](http://dx.doi.org/10.1016/0162-0134(84)85038-2).

564 Cullen, W.R., Reimer, K.J., 1989. Arsenic speciation in the environment. Chem. Rev. 89,
565 713-764.

566 Czarnecki, G.L., Baker, D.H., Garst, J.E., 1984. Arsenic-Sulfur Amino Acid Interactions in
567 the Chick. J. Anim. Sci. 59, 1573-1581. <https://doi.org/10.2527/jas1984.5961573x>.

568 D'Angelo, E., Zeigler, G., Beck, E.G., Grove, J., Sikora, F., 2012. Arsenic species in broiler
569 (*Gallus gallus domesticus*) litter, soils, maize (*Zea mays* L.), and groundwater from litter-
570 amended fields. Sci. Total Environ. 438, 286-292.
571 <http://dx.doi.org/10.1016/j.scitotenv.2012.08.078>.

572 Delnomdedieu, M., Basti, M.M., Otvos, J.D., Thomas, D.J., 1993. Transfer of Arsenite from
573 Glutathione to Dithiols: A Model of Interaction. Chem. Res. Toxicol. 6, 598-602.

574 Dilda, P.J., Hogg, P.J., 2007. Arsenical-based cancer drugs. Cancer Treat. Rev. 33, 542-564.
575 <http://dx.doi.org/10.1016/j.ctrv.2007.05.001>.

576 Dill, K., Adams, E.R., O'Connor, R.J., McGown, E.L., 1987. 2D NMR studies of the
577 phenyldichloroarsine—british anti—lewisite adduct. Magn. Reson. Chem. 25, 1074-1077.
578 <http://dx.doi.org/10.1002/mrc.1260251211>.

579 Dill, K., Huang, L., Bearden, D.W., McGown, E.L., O'Connor, R.J., 1991. Activation
580 energies and formation rate constants for organic arsenical-antidote adducts as determined by
581 dynamic NMR spectroscopy. Chem. Res. Toxicol. 4, 295-299.
582 <http://dx.doi.org/10.1021/tx00021a006>.

583 Doerge, D.R., Twaddle, N.C., Churchwell, M.I., Beland, F.A., 2020. Reduction by, ligand
584 exchange among, and covalent binding to glutathione and cellular thiols link metabolism and
585 disposition of dietary arsenic species with toxicity. Environ. Int. 144, 106086.
586 <https://doi.org/10.1016/j.envint.2020.106086>.

587 Dringen, R., Spiller, S., Neumann, S., Koehler, Y., 2016. Uptake, Metabolic Effects and
588 Toxicity of Arsenate and Arsenite in Astrocytes. Neurochemical Research 41, 465-475.
589 <https://doi.org/10.1007/s11064-015-1570-9>.

590 Farrugia, L., 1997. ORTEP-3 for Windows - a version of ORTEP-III with a Graphical User
 591 Interface (GUI). *J. Appl. Crystallogr.* 30, 565.
 592 <http://dx.doi.org/10.1107/S0021889897003117>.

593 Friedheim, E.A.H., da Silva, J.R., Martins, A.V., 1954. Treatment of Schistosomiasis
 594 Mansoni with Antimony-a, a'-Dimercapto-Potassium Succinate (TWSb). *Am. J. Trop. Med.*
 595 *Hyg.* 3, 714-727.

596 Gong, Z., Jiang, G., Cullen, W.R., Aposhian, H.V., Le, X.C., 2002. Determination of Arsenic
 597 Metabolic Complex Excreted in Human Urine after Administration of Sodium 2,3-
 598 Dimercapto-1-propane Sulfonate. *Chem. Res. Toxicol.* 15, 1318-1323.
 599 <http://dx.doi.org/10.1021/tx020058m>.

600 Guha Mazumder, D.N., 2003. Chronic Arsenic Toxicity: Clinical Features, Epidemiology,
 601 and Treatment: Experience in West Bengal. *J. Environ. Sci. Health, Part A: Toxic/Hazard.*
 602 *Subst. Environ. Eng.* 38, 141-163. <http://dx.doi.org/10.1081/ESE-120016886>.

603 Heinrich-Ramm, R., Schaller, K.H., Horn, J., Angerer, J., 2003. Arsenic species excretion
 604 after dimercaptopropanesulfonic acid (DMPS) treatment of an acute arsenic trioxide
 605 poisoning. *Arch. Toxicol.* 77, 63 - 68. <https://doi.org/10.1007/s00204-002-0413-z>.

606 Huckerby, T.N., Tudor, A.J., Dawber, J.G., 1985. Acid-base studies of glutathione (L-
 607 [gamma]-glutamyl-L-cysteinyl-L-glycine) by one- and two-dimensional nuclear magnetic
 608 resonance spectroscopy. *J. Chem. Soc., Perkin Trans. 2*, 759-763.
 609 <http://dx.doi.org/10.1039/P29850000759>.

610 Karplus, M., 1963. Vicinal Proton Coupling in Nuclear Magnetic Resonance. *J. Am. Chem.*
 611 *Soc.* 85, 2870-2871. <http://dx.doi.org/10.1021/ja00901a059>.

612 Kaviani, S., Shahab, S., Sheikhi, M., Ahmadianarog, M., 2019. DFT study on the selective
 613 complexation of meso-2,3-dimercaptosuccinic acid with toxic metal ions (Cd²⁺, Hg²⁺ and
 614 Pb²⁺) for pharmaceutical and biological applications. *J. Mol. Struct.* 1176, 901-907.
 615 <https://doi.org/10.1016/j.molstruc.2018.09.027>.

616 Kretzschmar, J., Brendler, E., Wagler, J., Schmidt, A.-C., 2014. Kinetics and activation
 617 parameters of the reaction of organoarsenic(V) compounds with glutathione. *J. Hazard.*
 618 *Mater.* 280, 734-740. <http://dx.doi.org/10.1016/j.jhazmat.2014.08.036>.

619 Leermakers, M., Baeyens, W., De Gieter, M., Smedts, B., Meert, C., De Bisschop, H.C.,
 620 Morabito, R., Quevauviller, P., 2006. Toxic arsenic compounds in environmental samples:
 621 Speciation and validation. *Trends Anal. Chem.* 25, 1-10.
 622 <http://dx.doi.org/10.1016/j.trac.2005.06.004>.

623 Liang, Y., Shi, J., Chen, L., Ding, G., 1980. Dimercaptosuccinic acid per os promoted the
 624 excretions of Pb, Cu, Sb, Sr, Tl, and Pm. *Acta Pharmacol. Sin.* 15, 335-340.

625 López-Moreno, S., Errandonea, D., Pellicer-Porres, J., Martínez-García, D., Patwe, S.J.,
 626 Achary, S.N., Tyagi, A.K., Rodríguez-Hernández, P., Muñoz, A., Popescu, C., 2018. Stability
 627 of FeVO₄ under Pressure: An X-ray Diffraction and First-Principles Study. *Inorg. Chem.* 57,
 628 7860-7876. <https://doi.org/10.1021/acs.inorgchem.8b00984>.

629 Lu, P.H., Tseng, J.C., Chen, C.K., Chen, C.H., 2017. Survival without peripheral neuropathy
630 after massive acute arsenic poisoning: Treated by 2,3-dimercaptopropane-1-sulphonate. J.
631 Clin. Pharm. Ther. 42, 506-508. <https://doi.org/10.1111/jcpt.12538>.

632 McCann, M.S., Maguire-Zeiss, K.A., 2021. Environmental toxicants in the brain: A review of
633 astrocytic metabolic dysfunction. Environ. Toxicol. Pharmacol. 84, 103608.
634 <https://doi.org/10.1016/j.etap.2021.103608>.

635 Miller Jr, W.H., Schipper, H.M., Lee, J.S., Singer, J., Waxman, S., 2002. Mechanisms of
636 action of arsenic trioxide. Cancer Res. 62, 3893-3903.

637 Niemikoski, H., Koske, D., Kammann, U., Lang, T., Vanninen, P., 2020. Studying the
638 metabolism of toxic chemical warfare agent-related phenylarsenic chemicals in vitro in cod
639 liver. J. Hazard. Mater. 391, 122221. <https://doi.org/10.1016/j.jhazmat.2020.122221>.

640 Nualláin, C.Ó., Cinnéide, S.Ó., 1973. The thermodynamic ionization constants of aromatic
641 arsonic acids. J. Inorg. Nucl. Chem. 35, 2871-2881. [http://dx.doi.org/10.1016/0022-](http://dx.doi.org/10.1016/0022-1902(73)80519-6)
642 [1902\(73\)80519-6](http://dx.doi.org/10.1016/0022-1902(73)80519-6).

643 Nurchi, V.M., Buha Djordjevic, A., Crisponi, G., Alexander, J., Bjørklund, G., Aaseth, J.,
644 2020. Arsenic Toxicity: Molecular Targets and Therapeutic Agents. Biomolecules 10.
645 <https://doi.org/10.3390/biom10020235>.

646 O'Connor, R.J., McGown, E.L., Dill, K., Hallowell, S.F., 1989. Two-dimensional NMR
647 studies of arsenical-sulphydryl adducts. Magn. Reson. Chem. 27, 669-675.
648 <http://dx.doi.org/10.1002/mrc.1260270713>.

649 Pergantis, S.A., Cullen, W.R., Chow, D.T., Eigendorf, G.K., 1997. Liquid chromatography
650 and mass spectrometry for the speciation of arsenic animal feed additives. J. Chromatogr. A
651 764, 211-222. [http://dx.doi.org/10.1016/S0021-9673\(96\)00914-4](http://dx.doi.org/10.1016/S0021-9673(96)00914-4).

652 Persistence of Vision Pty. Ltd. Persistence of Vision Raytracer (Version 3.6). Retrieved from
653 <http://www.povray.org/download/>, 2004.

654 Petrunkin, V.E., 1956. Synthesis and Properties of Dimercapto Derivatives of Alkylsulfonic
655 Acid. Ukr. Khim. Zh. 22, 603-607.

656 Pitten, F.A., Müller, G., König, P., Schmidt, D., Thurow, K., Kramer, A., 1999. Risk
657 assessment of a former military base contaminated with organoarsenic-based warfare agents:
658 uptake of arsenic by terrestrial plants. Sci. Total Environ. 226, 237-245.
659 [http://dx.doi.org/10.1016/S0048-9697\(98\)00400-8](http://dx.doi.org/10.1016/S0048-9697(98)00400-8).

660 Ray, A., Shelly, A., Roy, S., Mazumder, S., 2020. Arsenic induced alteration in Mrp-1 like
661 activity leads to zebrafish hepatocyte apoptosis: The cellular GSH connection. Environ.
662 Toxicol. Pharmacol. 79, 103427. <https://doi.org/10.1016/j.etap.2020.103427>.

663 Roerdink, A.R., Aldstadt, J.H., 2005. Sequential injection absorption spectrophotometry
664 using a liquid-core waveguide: Determination of p-arsanilic acid in natural waters. Anal.
665 Chim. Acta 539, 181-187. <http://dx.doi.org/10.1016/j.aca.2005.02.067>.

666 Sattar, A., Xie, S., Hafeez, M.A., Wang, X., Hussain, H.I., Iqbal, Z., Pan, Y., Iqbal, M.,
667 Shabbir, M.A., Yuan, Z., 2016. Metabolism and toxicity of arsenicals in mammals. *Environ.*
668 *Toxicol. Pharmacol.* 48, 214-224. <https://doi.org/10.1016/j.etap.2016.10.020>.

669 Sheldrick, G., 2008. A short history of SHELX. *Acta Crystallogr., Sect. A: Found.*
670 *Crystallogr.* 64, 112-122. <http://dx.doi.org/10.1107/S0108767307043930>.

671 Sheldrick, G.M., SHELXS-97, A Computer Program for the Solution of Crystal Structures,
672 Version: WinGX©, 1986-1997, Release 97-2; G. M. Sheldrick, SHELXL97, A Computer
673 Program for Crystal Structure Refinement, Version: WinGX©, 1993-1997, Release 97-2.

674 Stock, T., 1996. Sea-Dumped Chemical Weapons and the Chemical Weapons Convention, in:
675 Kaffka, A.V. (Ed.), *Sea-Dumped Chemical Weapons: Aspects, Problems and Solutions*.
676 Springer Netherlands, pp. 49-66.

677 Stock, T., Lohs, K., 1997. Part II. Chemical warfare agents and munition and toxic armament
678 wastes, in: Stock, T., Lohs, K. (Eds.), *The Challenge of Old Chemical Munitions and Toxic*
679 *Armament Wastes*. Oxford University Press, Oxford.

680 Sun, B., Macka, M., Haddad, P.R., 2002. Separation of organic and inorganic arsenic species
681 by capillary electrophoresis using direct spectrophotometric detection. *Electrophoresis* 23,
682 2430-2438. [http://dx.doi.org/10.1002/1522-2683\(200208\)23:15<2430::AID-](http://dx.doi.org/10.1002/1522-2683(200208)23:15<2430::AID-ELPS2430>3.0.CO;2-F)
683 [ELPS2430>3.0.CO;2-F](http://dx.doi.org/10.1002/1522-2683(200208)23:15<2430::AID-ELPS2430>3.0.CO;2-F).

684 Suzuki, S., Arnold, L.L., Pennington, K.L., Kakiuchi-Kiyota, S., Chen, B., Lu, X., Le, X.C.,
685 Cohen, S.M., 2012. Effects of co-administration of dietary sodium arsenate and 2,3-
686 dimercaptopropane-1-sulfonic acid (DMPS) on the rat bladder epithelium. *Toxicology* 299,
687 155-159. <http://dx.doi.org/10.1016/j.tox.2012.05.019>.

688 Tørnes, J.A., Opstad, A.M., Johnsen, B.A., 2006. Determination of organoarsenic warfare
689 agents in sediment samples from Skagerrak by gas chromatography-mass spectrometry. *Sci.*
690 *Total Environ.* 356, 235-246. <http://dx.doi.org/10.1016/j.scitotenv.2005.03.031>.

691 von Döllen, A., Strasdeit, H., 1998. Models for the Inhibition of Dithiol-Containing Enzymes
692 by Organoarsenic Compounds: Synthetic Routes and the Structure of [PhAs(HlipS2)]
693 (HlipS22- = Reduced Lipoic Acid). *Eur. J. Inorg. Chem.* 1998, 61-66.

694 Wisessaowapak, C., Visitnonthachai, D., Watcharasit, P., Satayavivad, J., 2021. Prolonged
695 arsenic exposure increases tau phosphorylation in differentiated SH-SY5Y cells: The
696 contribution of GSK3 and ERK1/2. *Environ. Toxicol. Pharmacol.* 84, 103626.
697 <https://doi.org/10.1016/j.etap.2021.103626>.

698